Support and challenges to the melanosomal casing model based on nanoscale distribution of metals within iris melanosomes detected by X-ray fluorescence analysis

T. Gorniak[1,2,3], *T. Haraszti*[2,4], *H. Suhonen*[5], *Y. Yang*[6], *A. Hedberg-Buenz*[7,8], *D. Koehn*[7], *R. Heine*[6], *M. Grunze*[1,2], *A. Rosenhahn*[1,2,3*], *and M.G. Anderson*[7,8*]

[1] *Institute of Functional Interfaces (IFG), Karlsruhe Institute of Technology (KIT), Hermann-von-Helmholtz-Platz 1, 76344 Eggenstein-Leopoldshafen, Germany*
[2] *Applied Physical Chemistry, Ruprecht-Karls-University Heidelberg, Im Neuenheimer Feld 253, 69120 Heidelberg, Germany*
[3] *Analytical Chemistry - Biointerfaces, Ruhr-University Bochum, NC 4/27, 44780 Bochum, Germany*
[4] *Max-Planck-Institut for Intelligent Systems, Heisenbergstr. 3, 70569 Stuttgart, Germany*
[5] *ESRF, 6 rue Jules Horowitz, BP 220, F-38043 Grenoble Cedex, France*
[6] *Institute for Photon Science and Synchrotron Radiation (IPS), Karlsruhe Institute of Technology (KIT), Hermann-von-Helmholtz-Platz 1, 76344 Eggenstein-Leopoldshafen, Germany*
[7] *Department of Molecular Physiology and Biophysics, The University of Iowa, Iowa City, IA 52242, USA*
[8] *Center for the Prevention and Treatment of Visual Loss, Iowa City Veterans Affairs (VA) Health Care System, Iowa City, IA 52246, USA*

*These authors contributed equally to this work.
Correspondance should be addressed to
M.G. Anderson (michael-g-anderson@uiowa.edu)
and A. Rosenhahn (axel.rosenhahn@rub.de)

Supporting information S1

Sample preparation

This study was carried out in strict accordance with the recommendations in the Guide for the Care and Use of Laboratory Animals of the National Institutes of Health. The protocol was approved by the Institutional Animal Care and Use Committee of the University of Iowa (Animal Protocol 1006131). All mice were euthanized in accordance to the "AVMA guidelines on Euthanasia".

Iridial melanosomes from 6-week old C57BL/6J and DBA/2J mice were purified by sucrose gradient purification (Anderson et al. 2006, Gahl et al. 1995, Seiji et al. 1963), vitrified, and subsequently freeze-dried as previously described (Gorniak et al. 2014). In brief, following cervical dislocation to the animal, irides were dissected in ice-cold buffer (pH 7.2, 10 mM HEPES and 0.25 M sucrose) and homogenized in a 7 ml Dounce glass:glass homogenizer (Kimble-Kontes) using 50 strokes of the A pestle and 30 strokes of the B pestle. Following centrifugation at $800\,g$ for 10 min at a temperature of 5 °C, the supernatant – containing the melanosomes – was removed and centrifuged at $15\,000\,g$ for 15 min. Pelleted organelles were resuspended in fresh buffer, which was put on a layered sucrose gradient (2.0 M sucrose at the bottom of the vial, passing 1.8 M, 1.6 M, 1.55 M, 1.5 M, 1.4 M, 1.2 M and reaching 1.0 M at the top) for a final purification step that involved centrifuging at $100\,000\,g$ for 1 h at 5 °C. Finally, the supernatant was removed and the pelleted organelles were resuspended in fresh buffer for storage and further experimental usage. The organelles extracted from each mouse strain were pooled separately. Hence, each sample volume used for the experiment comprised a mixture of melanosomes from 8 animals belonging to a group of the same strain and age.

Ideally, cryo-fixed specimen should be used in order to preserve the melanosomes' physiological state during the experiment as good as possible. The experimental end-station used for this study, however, did not

provide the infrastructure to perform the measurements within an evacuated and cryogenic sample environment. Hence, we used dehydrated organelles as second best option. To achieve this, we utilized vitrification followed by freeze-drying. Prior to the fixative step by vitrification, purified melanosomes were washed with Milli-Q^{TM} water. This was necessary because we found that during dehydration by sublimation of the amorphous ice within the cryogenic specimen, the remaining components present in the buffer solution build up a tension force, and as consequence, typically disrupt the fragile carbon nanosheets. In order to remove the problematic constituents, we applied the following washing protocol. Starting with $10\,\mu$l of melanosome suspension, $30\,\mu$l, $120\,\mu$l and $800\,\mu$l of Milli-Q^{TM} water were successively added at 15 min increments. The resulting diluted suspension was centrifuged at $14\,000\,g$ for 15 min at a temperature of $5\,^{\circ}$C and the supernatant was removed. Finally, the pelleted melanosomes were resuspended in pure Milli-Q^{TM} water and immediately cryo-fixed. For this, $4\,\mu$l of melanosome suspension was pipetted onto a TEM-grid (Cu mesh with a 200 spacing covered by a holey carbon C-flat^{TM} film with a 2/4 perforation, Protochips Inc., USA). After blotting the water with cellulose paper (grade No. 1, Whatman^{TM}, USA) the sample was quickly dipped (Kasas et al. 2003) into a liquid mixture containing $37\,\%$ of ethane and $63\,\%$ of propane (Tivol et al. 2008) at approximately 80 K using a semi-automatic plunge-freezing apparatus. Subsequently, the cryo-fixed samples were stored in liquid nitrogen until further processing. In the final preparation step, the vitrified specimens were freeze-dried, using a sublimation pressure of 1×10^{-8} mbar within a vacuum chamber warmed from 80 K to 300 K over 48 h.

Use of titanium dissection tools in extraction and sample preparation prevented metal contamination. To avoid parasitic Cu signals from the TEM-grid, the melanosome suspension never had direct contact with it. Prior to imaging, the exposed surface was covered with a metal-free Kapton adhesive, and the Cu support was removed, leaving the melanosomes sandwiched between the 20-nm thin carbon-sheet of the TEM-grid and the Kapton substrate.

X-ray fluorescence analysis

At beamline ID22NI of the ESRF, a photon energy of $E_{\mathrm{ph}} = 17\,\mathrm{keV}$ was selected to excite K-level emission lines of Zn, Ca and Cu (Hong & Simon 2007). The photons were focused to a spot measuring $(73 \times 71)\,\mathrm{nm}$ full width at half maximum (FWHM) in horizontal and vertical directions, respectively. The photon flux in the KB focus was $8.94 \times 10^{10}\,\mathrm{s}^{-1}$. For data acquisition the samples were raster-scanned with a pitch of $100\,\mathrm{nm}$ and a dwell time of $0.1\,\mathrm{s}$. The emitted X-ray fluorescence signal was recorded with a silicon drift detector (Vortex-EX, SII NanoTechnology Inc., USA) positioned $6\,\mathrm{mm}$ away from the sample. The angle between the detected radiation and the incident beam was 75°. Following imaging, spatial distributions of single elements were visualized using PyMCA software in the version 4.6.2 (Solé et al. 2007).

At room temperature the impact of radiation damage is usually less of an issue for dehydrated samples than it is for hydrated biological material because contributions from radiolysis of water (Schneider 1998) can be neglected. Here, the photon flux was adjusted with aluminum attenuators such that no visible alteration of the sample during scanning could be detected under the optical beamline microscope. Furthermore, the depicted sample regions were scanned only once.

Measuring photon flux with a photo diode allowed us to normalize data and account for changes in the incident beam intensity. We also corrected for the effect of detector dead times. Quantification of the XRF results in terms of mass per projected unit area was achieved by using standard samples from the National Institute of Standards and Technology (NIST). Dried bovine liver (NIST, SRM1577B) and a silica-based glass film (NIST, SRM1832) were used to calibrate the measurements in order to calculate the quantities of Zn, Ca and Cu present in single melanosomes.

Metal concentrations observed in this study (typically $1 \times 10^{-8}\,\mu\mathrm{g}\,\mu\mathrm{m}^{-2}$ for Ca and $1 \times 10^{-9}\,\mu\mathrm{g}\,\mu\mathrm{m}^{-2}$ for both Cu and Zn) can also be expressed in terms of number of atoms per unit area. Considering the corresponding atomic masses, one gets the following atomic number densities: $1.50 \times 10^{8}\,\mu\mathrm{m}^{-2}$, $9.48 \times 10^{6}\,\mu\mathrm{m}^{-2}$ and $9.21 \times 10^{6}\,\mu\mathrm{m}^{-2}$ for Ca, Cu and Zn, respectively. These numbers can also be translated into an estimate of metal atoms detected per illuminated area. Taking the size of the nanofocus into account, the resulting atomic numbers per illuminated area are 7.79×10^{5}, 4.91×10^{4} and 4.77×10^{4} for Ca, Cu and Zn, respectively.

The sensitivity of the instrument at beamline ID22NI can be regarded to be 1 ppm, which means that traces of an element are potentially detectable as soon as every millionth atom of the sample can be attributed

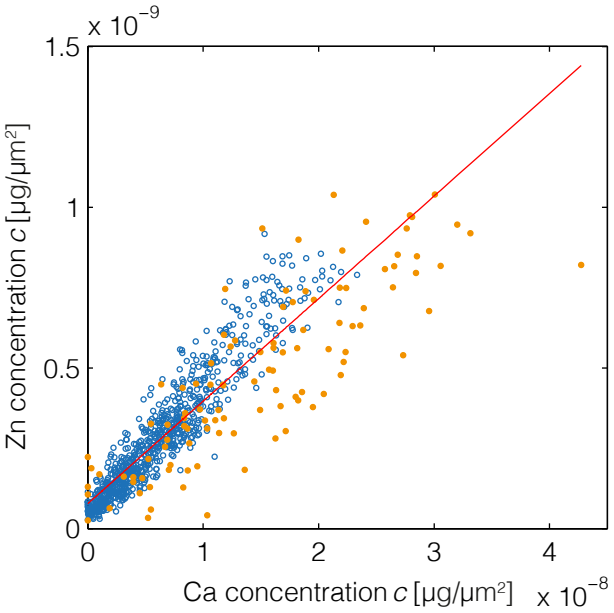

Figure S1 – Correlative metal distributions within single melanosomes. Scatter plots of Zn and Ca concentrations in purified iridial melanosomes from C57BL/6J (*orange discs*) and DBA/2J (*blue circles*) mice. The concentrations of Zn and Ca show a positive correlation across all melanosomes. The applied linear regression analysis to both datasets combined (*red line*) yields a slope of $m_{\mathrm{total}} = 0.032$. Treated separately, the fits generate the slopes $m_{\mathrm{orange}} = 0.026$ and $m_{\mathrm{blue}} = 0.039$ for the C57BL/6J and DBA/2J datasets, respectively. The calculated correlation coefficient for the combined dataset is $r_{\mathrm{total}} = 0.91$. Hence, all results described earlier in the context of a correlation Cu vs. Ca are also valid in the context of Cu vs. Zn.

to the species of interest. This information can be put into perspective with the results given above. Making a simplified assumption that our organic sample solely consists of carbon, and a typical organelle size is 1 µm, one can expect to find 5.87×10^8 C atoms inside an illuminated volume of $(73 \times 71 \times 1000)\,\mathrm{nm}$. Assuming a sensitivity of 1 ppm, about 600 metal atoms suffice to be present within the nanofocus to be detectable. Hence, the concentrations and atomic numbers revealed in this study lie at least a factor of 100 above the sensitivity threshold of the instrument used.

The calculation of the concentrations' error margins (20 % for Zn, 12 % for Ca and 25 % for Cu) is based on two contributions, first, the concentration uncertainties inherent to the standard samples as tabulated by the NIST and second, the actual inhomogeneity across the reference samples as determined by XRF scans. Assuming an organelle to entirely consist of melanin ($C_{25}O_{13}N_3H_9$) with a density of $\varrho = 1.25\,\mathrm{g\,cm^{-3}}$,* the absorption lengths μ_{a} at the excitation energy E_{ex} and the lowest fluorescence energy $E_{\mathrm{Ca}} = 3.69\,\mathrm{keV}$ are 10.5 mm and 0.1 mm, respectively (Henke et al. 1993). These numbers result in the attenuation values $A_{\mathrm{ex}} = 9.5 \times 10^{-5}$ and $A_{\mathrm{Ca}} = 9.5 \times 10^{-3}$ at a relevant length scale of $d = 1$ µm (organelle size in beam direction). Hence, we can exclude primary and secondary absorption to play a significant role in this study.

The RGB images in Figure 1 as well as the scatter plots in Figure 2 for metal correlation analysis are based on data points that have been extracted from XRF maps by segmentation, i.e. the separation of single melanosomes from the background. The segmentation rule was as follows: Calculate the mean background signal $\overline{m}$ and its standard deviation σ in the Cu channel within an area free of melanosomes and exclude all pixels whose intensity falls below the threshold value $\tau = \overline{m} + 35\sigma$. The factor of 35 was chosen as passing this number the last pixel from the background signal not connected to single melanosomes disappeared. The results were further refined with the application of basic built-in MATLAB functions for segmentation (imdilate, imfill, edge, imerode and imclearborder).

*Three orientation guides contribute to this estimate. First, during the purification of the melanosomes by a sucrose column, they pass a layer of 2 M sucrose solution with a density of $1.25\,\mathrm{g\,cm^{-3}}$. Second, our own unpublished transmission X-ray microscopy data yields values of about $1.30\,\mathrm{g\,cm^{-3}}$ for hydrated organelles. Third, sepia melanin granules have previously been reported to have a density of $1.68\,\mathrm{g\,cm^{-3}}$ (Zeise et al. 1990).

Correlation between Zn and Ca

To demonstrate that all results discussed in the context of a correlation between Cu and Ca are also valid for the pair Cu/Zn, as stated in the manuscript, Figure S1 shows a scatter plot of Zn and Ca data. The graph illustrates a positive correlation between these two metals. With a correlation coefficient of $r_{\mathrm{total}} = 0.91$, the occurrence of the two metals can be regarded as highly correlated.

References

Anderson, M. G., Haraszti, T., Petersen, G. E., Wirick, S., Jacobsen, C., John, S. W. M. & Grunze, M. (2006), 'Scanning transmission X-ray microscopic analysis of purified melanosomes of the mouse iris', *Micron* **37**(8), 689–698.

Gahl, W. A., Potterf, B., Durham Pierre, D., Brilliant, M. H. & Hearing, V. J. (1995), 'Melanosomal Tyrosine Transport in Normal and Pinkeyed Dilution Murine Melanocytes', *Pigment Cell Research* **8**(5), 229–233.

Gorniak, T., Haraszti, T., Garamus, V. M. & Buck, A. R. (2014), 'Nano-Scale Morphology of Melanosomes Revealed by Small-Angle X-Ray Scattering', *PLoS ONE* **9**(3), e90884.

Henke, B., Gullikson, E. M. & Davis, J. (1993), 'X-Ray Interactions: Photoabsorption, Scattering, Transmission, and Reflection at E = 50-30,000 eV, Z = 1-92', *Atomic Data and Nuclear Data Tables* **54**(2), 181–342.

Hong, L. & Simon, J. D. (2007), 'Current understanding of the binding sites, capacity, affinity, and biological significance of metals in melanin.', *The Journal of Physical Chemistry B* **111**(28), 7938–7947.

Kasas, S., Dumas, G., Dietler, G., Catsicas, S. & Adrian, M. (2003), 'Vitrification of cryoelectron microscopy specimens revealed by high-speed photographic imaging', *Journal of Microscopy* **211**(1), 48–53.

Schneider, G. (1998), 'Cryo X-ray microscopy with high spatial resolution in amplitude and phase contrast', *Ultramicroscopy* **75**(2), 85–104.

Seiji, M., Fitzpatrick, T. B. & Simpson, R. T. (1963), 'Chemical composition and terminology of specialized organelles (melanosomes and melanin granules) in mammalian melanocytes'.

Solé, V., Papillon, E., Cotte, M., Walter, P. & Susini, J. (2007), 'A multiplatform code for the analysis of energy-dispersive X-ray fluorescence spectra', *Spectrochimica Acta Part B: Atomic Spectroscopy* **62**(1), 63–68.

Tivol, W. F., Briegel, A. & Jensen, G. J. (2008), 'An Improved Cryogen for Plunge Freezing', *Microscopy and Microanalysis* **14**(05).

Zeise, L., Addison, R. B. & Chedekel, M. R. (1990), 'Bio-analytical Studies of Eumelanins. I. Characterization of Melanin the Particle', *Pigment Cell Research* **3**, 48–53.